Minimising Oil Droplet Size using Ultrasonic Emulsification

By

T. S. H. Leong[a], T. J. Wooster[b], S. E. Kentish[a]*, M. Ashokkumar[a]

[a]Particulate Fluids Processing Centre, Department of Chemical and Biomolecular Engineering & School of Chemistry, University of Melbourne, Parkville, Victoria 3010, Australia

[b]Food Science Australia, Private Bag 16, Werribee Victoria 3030, Australia

Abstract

The efficient production of nanoemulsions, with oil droplet sizes of less than 100 nm would facilitate the inclusion of oil soluble bioactive agents into a range of water based foods. Small droplet sizes lead to transparent emulsions so that product appearance is not altered by the addition of an oil phase. In this paper, we demonstrate that it is possible to create remarkably small transparent O/W nanoemulsions with average diameters as low as 40 nm from sunflower oil. This is achieved using ultrasound or high shear homogenization and a surfactant/co-surfactant/oil system that is well optimized. The minimum droplet size of 40 nm, was only obtained when both droplet deformability (surfactant design) and the applied shear (equipment geometry) were optimal. The time required to achieve the minimum droplet size was also clearly affected by the equipment configuration. Results at atmospheric pressure fitted an expected exponential relationship with the total energy density. However, we found that this relationship changes when an overpressure of up to 400 kPa is applied to the sonication vessel, leading to more efficient emulsion production. Oil stability is unaffected by the sonication process.

Keywords

Ultrasound, emulsification, nanoemulsions, triglyceride, surfactants

***Corresponding Author**
Address: Department of Chemical and Biomolecular Engineering, University of Melbourne, Parkville, Victoria 3010, Australia. Phone: +61 3 8344 8862 Fax: +61 3 8344 4153
E-mail address: sandraek@unimelb.edu.au

Introduction

Nanoemulsions are colloidal dispersions comprising two immiscible liquids, one of which is dispersed in the other, with droplet sizes between 20 and 200 nm [1, 2]. The small droplet size implies that nanoemulsions flow easily, can be optically transparent and have unique texture/rheological properties [3, 4]. Nanoemulsions are also attractive from a product stability point of view; their very small size enhances their physical stability [1, 2]. These properties make them highly attractive for cosmetic products and in the food industry [3, 5, 6]. Specifically, nanoemulsions offer the potential to deliver high concentrations of oil soluble nutraceuticals or bio-active food supplements into a range of water based foodstuffs. If the emulsion droplet size is below the detection limit of the human eye (around 50 nm) then the emulsion can appear translucent and so the visual quality of the product is unaffected [7].

Typically, emulsions are prepared by physical shearing processes [8-10]. The ultimate size of a homogenized emulsion is determined by the balance between two opposing processes; droplet break-up and droplet re-coalescence [10]. The frequency of both processes is promoted by the intense shear that occurs within a high shear homogeniser such as the microfluidizer or ultrasonic transducer. Droplet break-up occurs when the applied shear is greater than the Laplace pressure of the emulsion. In the simple case of a low oil volume fraction and negligible continuous phase viscosity, Taylor predicts that the emulsion radius (r):

$$r \propto \frac{\gamma}{\eta_c \dot{\gamma}} \qquad (1)$$

where γ is the interfacial tension, η_c is the continuous phase viscosity and $\dot{\gamma}$ is the shear rate [10-12].

The surfactant plays a critical role in both droplet breakup and re-coalescence. The surfactant aids droplet break-up by lowering the interfacial tension which reduces the resistance to droplet deformation [10]. The most important role of the surfactant is to prevent the immediate re-coalescence of newly formed droplets by rapid adsorption to, and stabilization of, the newly formed interface. In this case having an excess of surfactant in the continuous phase capable of rapidly adsorbing to the interface is essential [10]. Invariably the requirements of both droplet break-up re-coalescence dictate that small molecule surfactants are the most suited to the formation of nanoemulsions (compared to macromolecular emulsifiers) because of their greater ability to rapidly adsorb to interfaces and their much lower dynamic interfacial tensions.

The efficiency of droplet break-up within a homogenizer is also controlled by the nature and intensity of the shear. In most homogenizers droplet break-up occurs as a result of turbulent flow [13]. Droplet break-up in turbulent flow occurs via the action of viscous or inertial stress on the emulsion droplet. Which of these stresses dominate depends on the size of the droplet relative to the smallest turbulent eddy.[1] The power density, (P_v, W/ml) the average energy dissipated per unit time and unit volume, is the main measure of the strength of the turbulence. The maximum sized droplet that can exist under a certain turbulent flow regime is given by Equation 2[10]:

$$d_{\max} = CP_v^{-2/5}\gamma^{3/5}\rho_c^{-1/5} \qquad (2)$$

where C is a constant and ρ_c is the mass density of the emulsion.

[1] A detailed review of droplet deformation under turbulent shear can be found in Walstra[10] and Vankova et al. [14]

The average droplet diameter achieved is clearly a function of the intensity of shear as expressed through the power density (P_v), but will also depend upon the residence time within this shear field, τ (s) [13]. Karbstein and Schubert[15] argued that this dependency between residence time and average size is due to uneven power density distribution in the dispersing zone. To account for this dependency, they introduced the concept of "energy density", which is the simple product of the power density and the residence time within the shear field, τ (s):

$$E_v = P_v \tau \qquad (3)$$

This parameter may also be described as the energy input per unit volume, or the specific energy input, E_v, (J/ml) [15-18]. The average droplet diameter can then be described by a simple exponential relationship[15]:

$$d_{av} = C.E_v^{-b} \qquad (4)$$

Arguably the most powerful homogenizer, the Microfluidizer™ has been the focus of much of the recent work on nanoemulsion formation [7, 13]. However, the Microfluidizer is very expensive and is prone to significant losses in efficiency due to high equipment wear rates. Ultrasonic homogenisers might prove a viable alternative to the Microfluidizer™ because they are easy to clean and are capable of achieving similar local power densities. In an ultrasonic system, physical shear is provided predominantly by the process of acoustic cavitation; the formation, growth and subsequent collapse of microbubbles caused by the pressure fluctuations of the acoustic wave. A collapse event causes extreme levels of highly localised turbulence – an implosion on a microscopic

scale. It is the accumulation of many thousands of these miniature implosions that forms the basis of ultrasonic homogenisation.

In a classical ultrasonic horn transducer, the cavitational bubble cloud and consequently the region of high intensity shear is focused in a small zone immediately adjacent to the transducer face. The spatial variation in the shear field can mean that power usage is relatively inefficient. This means that ultrasonic homogenization is currently only suitable for small batches [1, 15]. The performance of this process might be improved by increasing the homogeneity of the field as well as the average power density. In turn, these improvements may come from changes to equipment geometry [19, 20] or the use of higher amplitude sonotrodes [17].

Another approach is the use of a constant amplitude sonotrode at system pressures in excess of the ambient value. It is well known that increasing the external pressure increases the cavitation threshold within an ultrasonic field and thus fewer bubbles form. However, increasing the external pressure also increases the collapse pressure of cavitation bubbles [21-23]. This means that the collapse of the bubbles when cavitation occurs becomes stronger and more violent than when the pressure is at atmospheric conditions. As cavitation is the most important mechanism of power dissipation in a low frequency ultrasonic system, these changes in cavitational intensity can be related directly to changes in the power density.

Work by Henglein and Gutierrez[24] indicated that at low sonication amplitudes, the effect of the cavitation threshold was dominant and both the chemical yield and sonoluminescence arising from an acoustic field decreased with increasing pressure. Conversely, at higher amplitudes, the bubble collapse effects dominated and yields increased with increasing pressure. Similarly, Sauter *et al.*[25] find that low overpressures improve de-agglomeration of nanoparticles, whereas higher overpressures have a negative effect. Both Bondy and Sollner[23] and Behrend[18] observe an optimum in emulsification efficiency at an absolute pressure of around two atmospheres which can again be attributed to these competing effects.

The application of ultrasound to the creation of nanoemulsions has been considered in several works, however the droplet sizes achieved were generally above 200nm [26-30]. Therefore in the present paper we re-examine the ability of ultrasonic homogenisers to produce nanoemulsions. Our approach is to enhance droplet formation by examining both terms in the Taylor Equation (Equation 1), surfactant and shear. On the surfactant side we examine how surfactant synergy can aid droplet deformation. On the shear size we examine how equipment geometry can be improved and whether the specific energy input of the sonifier can be enhanced through overpressure. Finally, we confirm through High Performance Liquid Chromatography (HPLC) that the structure of the triglyceride oil is not damaged through the use of such intensive shear. Overall the goal is to enhance ultrasonic homogenization to the point where it is capable of producing true nanoemulsions.

Materials and Methods

Unless noted otherwise, emulsions were prepared with 5.6 wt% surfactant and 15 wt% of sunflower oil (Crisco, purchased from retail supermarkets) with the balance purified water (Millipore, MilliQ system). Three surfactants were trialed both individually and in combination; Tween 80, Span 80 and sodium dodecyl sulfate (SDS) (all from Sigma Aldrich). In some experiments, polyethylene glycol(PEG) of Molecular Weight 6000 (Chem Supply) and fresh canola oil (Crisco, purchased from retail supermarkets) was also used.

All emulsions were pre-emulsified in a 250 mL beaker using an Ultra-Turrax mixer (Janke and Kankel) run through a Variac auto transformer at a low shear rate to avoid excessive foaming, for 1 to 2 minutes. Droplet size after pre-mixing was in the range of 5-10 μm. Required volumes were then transferred to the appropriate cell using a transfer syringe. Sonication was performed at an amplitude of 30 micron using a Branson Digital Sonifier (Branson, Connecticut, Model No. 450, nominal power 400W) providing power via a transducer (No. 102C) to an externally threaded horn of diameter 12 mm (1/2 inch) and length 71 mm (Branson Part No.101-147-037). In this type of unit, the power delivered to the transducer and ultimately to the solution is automatically adjusted to ensure a constant amplitude. Temperature was controlled by the circulation of cooling water at 21 to 23 ^{o}C, depending on room temperature.

Most experiments were conducted by immersing the standard Branson ultrasonic probe in a 40 ml solution within a water jacketed glass cell of internal dimensions 43 mm diameter

by 66 mm height (manufactured in-house, see Figure 1a). However, experiments were also conducted using a variety of other equipment configurations around the same Branson Sonifier horn. These used a Flow-thru horn (Branson Part No. 101-135-022, see Figures 1b and 1c), a water jacketed, sealed atmosphere treatment chamber of 15 mm internal diameter and 90 mm height (Branson Part No. see Figure 1d) and a in-line continuous flow cell (Branson Part No. 101-146-171, see Figure 1e) with inner diameter of 28 mm, outer diameter 47.5mm and height of 107 mm. While this latter device is designed for continuous flow applications, in the present case it was used simply as a chamber that could readily be pressurized. Argon (BOC Gases) was used to provide an overpressure to the system. The power density (P_v) delivered to the solution using each of these configurations was determined by the standard calorimetric method [31]. Results are presented in Figure 2.

As a comparison, emulsions were also prepared using a Microfluidics M-110Y microfluidizer (MFIC Corporation, Newton, MA, USA) with a F20 Y 75 μm interaction chamber and H30 Z 200 μm auxiliary chamber inline. Emulsions were prepared by subjecting pre-emulsions to 5 passes at 1000 ± 50 Bar. Pre-emulsions were prepared using a Silverson rotor-stator mixer on its lowest speed setting for 2 minutes and had a average particle size $D_{3,2}$ of 7.2 ± 0.038 μm in a mono-modal distribution. A cooling coil was used on the microfluidizer which meant that the emulsions decreased from ~ 20^{o}C to 10^{o}C over the course of their preparation.

A Zetasizer Nano (Malvern Instruments) was used to analyze the particle size distribution of the finer emulsions formed. This device performs size measurements by Dynamic Light Scattering (DLS), which measures the Brownian motion of the particles and relates this to the particle size, on the premise that larger particles have slower motion. Calculations are based on the Stokes-Einstein Equation:

$$d_H = \frac{\kappa T}{3\pi\eta D} \qquad (5)$$

where d_H is the hydrodynamic diameter, D is the translational diffusion coefficient, κ = Boltzmann's Constant, T is the absolute temperature and η is the viscosity. A refractive index of 1.456 and absorbance of 0.01 was used. Sufficient dilution of the emulsions was required to reduce the effect of multiple scattering on the measurements. This was achieved by dilution of 100 μL of the emulsion sample to approximately 13 to 20 mL of solution, or until a laser light attenuation of between 8 and 10 was achieved. To limit the effect of thermal energy on the measurements, 3 repeat measurements were performed to allow for thermal equilibration, with the final set being used for analysis. Emulsion particle sizes are quoted as the intensity average diameter. For the coarser emulsions of particle size greater than 150 nm, the size was measured with laser light scattering using a Mastersizer 2000 (Malvern, Worcestershire, United Kingdom). Information about emulsion particle size was then obtained via a best fit between light scattering (Mie) theory and the measured light scattering pattern. Emulsion particle size results are an average of three measurements of two freshly prepared emulsions.

HPLC analysis was conduced on a Shimadzu LC 20 system, and conducted on a PVA-silica column (250 X 4.5 mm I.D., S5 μm, 12 nm) using an Evaporative Light Scattering

Detector (ELSD) and detection at 210 nm followed by 220 nm. Samples were eluted from the column using a tertiary gradient of 1% isopropanol in hexane, dichloromethane and methanol at a flow rate of 0.9 ml min^{-1}. Before HPLC analysis, emulsions were de-emulsified by freeze drying and the oil/surfactant mixture that was obtained was then dissolved in a 1:1 mixture of petroleum ether:diethylether. 1 ml of this sample was analysis by HPLC for triglyceride content and for the presence of monoglycerides, diglycerides and free fatty acids. The different peaks of triglyceride digestion were identified by running known standards, fatty acids – oleic acid, diglycerides – diolein and monoglycerides – monoolein which were obtained from Sigma-Aldrich as chromatography standard purity.

Results and Discussion

Surfactant System Optimisation

The resistance of an emulsion droplet to deformation is governed by the magnitude of its Laplace pressure, which is controlled by the interfacial tension of the surfactant. It has been known for many decades that co-surfactants and surfactant mixing can significantly change the interfacial tension of oil-water mixtures as a result of surfactant synergy [32]. In the present work we examined if the addition of a co-surfactant (Span 80) altered the particle size of emulsions primarily stabilized by Tween 80 (Figure 3). These surfactants were selected for study for two reasons i) the known surfactant synergy between them [33] and 2) because they are food safe, cheap and generally available. These experiments used 40mL samples sonicated for 10 minute durations in the sealed atmospheric chamber (Figure 1d).

The incorporation of an increasing amount of Span 80 caused a steady reduction in average emulsion size up to a Span content of ca 6 wt%. Above 6 wt% Span 80 the trend reverses and there is a steady increase in average emulsion size. The reduction in emulsion size is caused by the synergy that arises from having two surfactants with opposing HLB's/packing geometries. Tween 80 is a hydrophilic surfactant with an interfacial molecular area of 2.48 nm^2 whilst Span 80 is a hydrophobic surfactant with an interfacial molecular area of 0.46 nm^2 [33]. Incorporating increasing amounts of Span 80 into the emulsion interface increases surfactant packing and optimizes the preferential interfacial curvature which results in a reduced interfacial tension . However, incorporation of too much Span 80 makes the surfactant system too hydrophobic and less able to stabilise oil in water emulsions [33].

More dramatic improvements in average droplet sizes were achieved by reducing the amount of oil in the sample (see Figure 4). Oil weight fractions of 7.5wt% and below resulted in translucent emulsions, with an optimum oil weight fraction of 2.5wt% generating the smallest particle size, at around 40 nm. However at such low oil concentrations there is actually four times as much surfactant present as oil and such a high surfactant loading may not always be desired. Higher production costs would also be likely, since higher throughput is necessary to incorporate larger amounts of oil into the required product.

Parallel work using a microfluidizer indicated that a different combination of surfactants might produce better results. Figure 5 shows an example of this system, the addition of increasing amounts of polyethylene glycol (M_w ~ 6000 Da) to a 15 vol% triglyceride emulsion stabilized by 5.6 wt % sodium dodecylsulphate(SDS). The addition of polyethylene glycol to the SDS stabilized emulsion causes a steady decrease in emulsion size up to about 15 wt%. The origin of the particle size reduction is two fold [7]. Firstly the addition of polyethylene glycol to the aqueous phase reduces the difference in viscosity of the two phases. Reducing the differential viscosity (η_D/η_C) leads to a lowering of the critical Weber number and droplet break-up occurs more readily. Secondly SDS is know to interact with polyethylene glycol via an ion-dipole interaction [34]. Recent work by Wooster *et al* [7] has shown that this interaction creates a synergy between the SDS and the PEG that further aids droplet deformation, possibly by lowering interfacial tension and/or increasing the Gibbs elasticity. Again, the minimum droplet size achieved is a remarkably small 40 nm.

As shown in Figure 6, this combination of surfactants also produced excellent results when utilized with ultrasound, with a particle size again of around 40 nm after 20 minutes of processing in the glass cell. The emulsions formed had low polydispersity (see Figure 7) and could be stored at room temperature for many weeks, without significant changes in their appearance. The earlier work of Wooster *et al.* [7] examined the Ostwald ripening of these systems in detail and demonstrated that the insolubility of triglyceride oils in water provides a kinetic barrier to Ostwald ripening. Unfortunately, while this surfactant

system provides optimum droplet sizes at relatively high oil concentrations, it is not a food safe system and so could not be used in food applications.

Equipment Optimisation

In order to vary the shear intensity of the system, we examined a number of equipment geometries (Figure 1). In the first instance, we trialed pumping the emulsion mixture through a continuous flow-through horn specifically designed for emulsion manufacture (see Figure 1b). However, the low shear intensity and low residence times for which the fluid remained inside the horn depleted any advantage this may have had in sonicating the sample. The sonication appeared to have in fact, little impact upon the pre-homogenized samples, as the bulk of the emulsion mixtures were distributed in the 10µm range.

A second mode of operation was investigated using this horn, that being a reverse vortexing action where the tip of the horn was submerged into the emulsion reservoir (see Figure 1c). This mode of operation was essentially a batch type operation, with additional circulation of emulsion up through the horn tip. The circulation was achieved by the sonication process creating a pressure difference between the inside of the horn and the tip of the horn that dragged fluid upwards into the hollow core and back out the side outlets. Emulsions produced via this mode of operation were significantly improved compared with the method where emulsion was fed via a pump. The circulation of fluid in this mode was slower than that of pumping, enabling a longer residence time; and shear intensity was increased as both the central and external surfaces of the horn were in

contact with the emulsion. Particle sizes down to approximately 150 nm could be achieved with the Tween/Span system, whilst sizes down to 50 nm were produced with an SDS/PEG system (Figure 6). These sizes were still slightly larger than could be achieved with a standard horn in a glass cell. Calorimetric calibration (Figure 2) indicated that at the 50% output used in these experiments the standard horn provided P_v=0.9 W/ml while the flow-through horn delivered only P_v = 0.6 W/ml. Thus this arrangement was less efficient at delivering power to the system.

We also trialed batch emulsification using a more compact cell design, referred to by the manufacturer as a sealed chamber arrangement (Figure 1d). This featured a very narrow space between the horn tip and the vessel wall. The sample size was also smaller (15 ml in the sealed chamber versus 40 ml in the glass cell) so the power density applied was much greater (2.3 W/ml). Results in the case of using SDS/PEG in this arrangement were impressive with droplet sizes of 55 nm being achieved after very short residence times (less than 5 minutes) (see Figure 6). However, while the emulsification time could be shortened the ultimate droplet size that could be achieved was still independent of the equipment arrangement at around 40 nm. This is the same size that was achieved using a microfluidizer and may represent the absolute limit of size for these nanoemulsions.

A final approach involved a slightly different cell arrangement that could be pressurized (Figure 1e). In this case, increasing the overpressure clearly increased the power delivered to the emulsion (Figure 2). As can be seen in Figure 8, the overpressure also has a significant effect on the average particle size after one minute of sonication using

SDS-PEG. The application of an overpressure of 300kPa resulted in a significant reduction of particle size to 57 nm at a delivered power level of 2.3 W/ml. This compares favorably with the sealed chamber arrangement which delivered 86 nm after one minute, at an equivalent power density. Overpressures beyond 400 kPa were ineffective, with a lack of audible cavitational noise supporting our conclusion that cavitation had decreased to a minimal level at these higher pressures.

It is useful to present all the results discussed here for the SDS-PEG system in terms of the specific energy delivered to the emulsion (J/ml) as described by Equation 3. As shown in Figure 9, the data clearly fits the power law relationship defined in Equation 4. The data provides for a value of b=0.37 at atmospheric pressure which is consistent with the value of b=0.4 provided both by Walstra[10] for ultrasonic emulsification and Karbstien and Schubert[15] for rotor-stator mixers. However, the use of overpressure appears to provide a nanoemulsion at a lower energy density than an atmospheric system. An emulsion of 50 nm droplet size can be prepared using around 160 J/ml if overpressure is applied, whereas around 500 J/ml is required at atmospheric pressure. This result is somewhat surprising; both Sauter et al.[25] and Behrend and Schubert[18] find that the effects of overpressure can be explained entirely in terms of the specific energy input, in which case the two curves should converge. However, Karbstein et al.[15] show similar results to those reported here when back pressure is applied to a high pressure mechanical homogenizer during the production of a rapeseed oil/water emulsion. Interestingly, the value of b=0.66 for overpressure also matches the value provided by Walstra[10] for

high pressure homogenization (b=0.6). This suggests some synergy in the use of high pressure for both operations.

Oil Stability

Given the sonication intensity applied to these emulsions we were somewhat concerned that we had perhaps damaged the structure of the triglyceride oil itself. The formation of diglycerides and monoglycerides as a result of triglyceride damage might be expected to facilitate emulsion formation as they have a lower interfacial tension than triglycerides. To assess if there was damage to the triglyceride, in particular the formation of surface active triglyceride hydrolysis products, analysis by HPLC was conducted. This showed that there was minimal production of free fatty acids, monoglycerides or diglycerides upon sonication. This is consistent with the results of Pandit and Joshi[35] who found that energy input levels of around 1000 J/ml were required for the hydrolysis of fatty oils by cavitation.

Conclusion

It has been demonstrated that ultrasound is a viable method for producing transparent nanoemulsions of triglyceride oils in water with mean particle sizes down to 40 nm. The smallest droplet size that can be achieved is fundamentally a function of the emulsion composition. Thus, 40 nm droplets could be achieved by altering the oil content of a triglyceride/Tween/Span combination or similarly by altering the PEG content in a triglyceride/SDS/PEG system. Achieving this minimum droplet size requires a certain

shear intensity, or power density as described by Equation 2. However, provided this is available, the minimum droplet size is independent of equipment configuration, with both ultrasonic systems and a Microfluidiser producing comparable results.

This work has confirmed the results of other authors that show that for shorter residence times, the droplet size of a specific surfactant mixture is controlled by the specific energy input. This specific energy is the simple product of the power delivered to the emulsion and the residence time. However, contrary to prior work, the relationship between this specific energy input and droplet size is different for emulsions produced at atmospheric pressure than those produced with an element of backpressure. The use of backpressure allows droplets of a given size to be formed at slightly lower specific energy levels. Finally, there is no evidence that such intense shear results in hydrolysis of the triglyceride oil.

Acknowledgements

Financial support for this work has been provided by both the University of Melbourne-CSIRO Collaborative Grant Scheme. Infrastructure support from both the Victorian Government Science Technology and Innovation Initiative and the Particulate Fluids Processing Centre, a Special Research Centre of the Australian Research Council is also gratefully acknowledged. Preliminary experiments and a literature review were completed by Bronwen Lee and Jan Zimak and their work is also acknowledged.

References

1. C. Solans, P. Izquierdo, J. Nolla, N. Azemar, and M.J. Garcia-Celma, *Nano-emulsions,* Current Opinion in Colloid & Interface Science 10 (2005) 102-110.
2. T. Tadros, R. Izquierdo, J. Esquena, and C. Solans, *Formation and stability of nano-emulsions,* Advances in Colloid and Interface Science 108-09 (2004) 303-318.
3. O. Sonneville-Aubrun, J.T. Simonnet, and F. L'Alloret, *Nanoemulsions: a new vehicle for skincare products,* Advances in Colloid and Interface Science 108-109 (2004) 145-149.
4. G.J. Nohynek, J. Lademann, C. Ribaud, and M.S. Roberts, *Grey goo on the skin? Nanotechnology, cosmetic and sunscreen safety,* Critical Reviews in Toxicology 37 (3) (2007) 251-277.
5. M. Schifone and H.S. Zadeh, *Cosmetic nanoemulsions,* Cosmetic Technology (Milano, Italy) 9 (7) (2006) 27-31.
6. S. Kentish, T.J. Wooster, M. Ashokkumar, S. Balachandran, R. Mawson, and L. Simons, *The Use of Ultrasonics for Nano-emulsion Preparation,* Innovative Food Science & Emerging Technologies 9 (2008) 170–175.
7. T.J. Wooster, P. Sanguansri, and M. Golding, *Impact of Oil Type on Nanoemulsion Formation and Ostwald Ripening Stability,* Langmuir 24 (22) (2008) 12758-12765.
8. E.S.R. Gopal, *Principles of emulsion formation,* in *Emulsion Science,* P. Sherman, Editor. 1968, Academic Press: New York. p. 1-75.
9. D.J. McClements, *Food Emulsions: Principles, Practices and Techniques*. 2nd ed. 2004, Washington, D. C.: CRC Press.
10. P. Walstra, *Principles of Emulsion Formation,* Chemical Engineering Science 48 (2) (1993) 333-349.
11. K. Meleson, S. Graves, and T.G. Mason, *Formation of concentrated nanoemulsions by extreme shear,* Soft Materials 2 (2-3) (2004) 109-123.
12. G.I. Taylor, *The formation of emulsions in definable fields of flow,* Proc. R. Soc. A146 (1934) 501.
13. S. Schultz, G. Wagner, K. Urban, and J. Ulrich, *High-Pressure Homogenization as a Process for Emulsion Formation,* Chem. Eng. & Tech. 27 (4) (2004) 361-368.
14. N. Vankova, S. Tcholakova, N.D. Denkov, I.B. Ivanov, V.D. Vulchev, and T. Danner, *Emulsification in turbulent flow - 1. Mean and maximum drop diameters in inertial and viscous regimes,* J. Colloid Inter. Sci 312 (2) (2007) 363-380.
15. H. Karbstein and H. Schubert, *Developments in the continuous mechanical production of oil-in-water macro-emulsions,* Chemical Engineering and Processing 34 (1995) 205-211.
16. B. Koglin, J. Pawlowski, and H. Schnoring, *Kontinuierliches Emulgieren mit Rotor/Stator-Maschinen: Einfluss der volumenbezognenen Dispergierleistung und der Verweizeit auft die Emulsionfeinheit,* Chem. Ing. Techn. 53 (8) (1981) 641-647.

17. B. Tal-Figiel, *The formation of stable W/O, O/W, W/O/W cosmetic emulsions in an ultrasonic field,* Chemical Engineering Research and Design 85 (A5) (2007) 730-734.
18. O. Behrend and H. Schubert, *Influence of hydrostatic pressure and gas content on continuous ultrasound emulsification,* Ultrasonics Sonochemistry 8 (3) (2001) 271-276.
19. P.R. Gogate, *Cavitational reactors for process intensification of chemical processing applications: A critical review,* Chemical Engineering and Processing 47 (4) (2008) 515-527.
20. P.R. Gogate, A.M. Wilhelm, and A.B. Pandit, *Some aspects of the design of sonochemical reactors,* Ultrasonics Sonochemistry 10 (6) (2003) 325-330.
21. K.E. Suslick, *Ultrasound*. 1988, Weinheim: VCH Publishers.
22. F.R. Young, *Cavitation*. 1989, London: McGraw-Hill.
23. C. Bondy and K. Sollner, *On the Mechanism of Emulsification by Ultrasonic Waves,* Transactions of the Faraday Society 31 (1935) 835-842.
24. A. Henglein and M. Gutierrez, *Sonochemistry and Sonoluminescence: Effects of External Pressure,* Journal of Physical Chemistry 97 (1993) 158-162.
25. C. Sauter, M.A. Emin, H.P. Schuchmann, and S. Tavman, *Influence of Hydrostatic Pressure and Sound Amplitude on the Ultrasound Induced Dispersion and De-agglomeration of Nano-particles,* Ultrasonics Sonochemistry 15 (2008) 517-523.
26. B. Abismail, J.P. Canselier, A.M. Wilhelm, H. Delmas, and C. Gourdon, *Emulsification by ultrasound: drop size distribution and stability,* Ultrasonics Sonochemistry 6 (1-2) (1999) 75-83.
27. S. Freitas, G. Hielscher, H.P. Merkle, and B. Gander, *Continuous contact- and contamination-free ultrasonic emulsification-a useful tool for pharmaceutical development and production,* Ultrasonics Sonochemistry 13 (1) (2006) 76-85.
28. S.M. Jafari, Y. He, and B. B., *Production of sub-micron emulsions by ultrasound and microfluidization techniques,* Journal of Food Engineering 82 (4) (2007) 478-488.
29. Y.F. Maa and C.C. Hsu, *Performance of Sonication and Microfluidization for Liquid-liquid Emulsification,* Pharmaceutical Development and Technology 4 (2) (1998) 233-240.
30. S.G. Gaikwad and A.B. Pandit, *Ultrasound Emulsification: Effect of ultrasonic and physicochemical properties on dispersed phase volume and droplet size,* ULtrasonics Sonochemistry 15 (2008) 554-563.
31. C.F. Ratoarinoro, A.M. Wilhelm, J. Berlan, and H. Delmas, *Power measurement in sonochemistry,* Ultrasonics Sonochemistry 2 (1) (1995) S43-S47.
32. J. Israelachvili, *The Science And Applications Of Emulsions - An Overview,* Colloids and Surfaces a-Physicochemical and Engineering Aspects 91 (1994) 1-8.
33. W.R. Liu, D.J. Sun, C.F. Li, Q. Liu, and H. Xu, *Formation and Stability of Paraffin Oil-in-Water Nano-Emulsions Prepared by the Emulsion Inversion Point Method,* Journal of Colloid and Interface Science 303 (2) (2006) 557-563.

34. J. Penfold, R.K. Thomas, and D.J.F. Taylor, *Polyelectrolyte/surfactant mixtures at the air-solution interface*, Curr. Opin. Colloid Interface Sci. 11 (6) (2006) 337-344.
35. A.B. Pandit and J.B. Joshi, *Hydrolysis of Fatty Oils by Cavitation*, Chemical Engineering Science 48 (19) (1993) 3440-3442.

Figure Captions

Figure 1 – Experimental set-up for the glass cell (a), the Flow-through horn (b and c), the sealed chamber (d), and the continuous flow attachment(e).

Figure 2 – The power delivered to the emulsion (P_v) for a range of equipment configurations and overpressure values.

Figure 3 – The effect of increasing Span 80 content on the average droplet diameter of 15 wt% O/W emulsions initially stabilized by 5.3 wt% Tween 80. 40mL samples were sonicated for 10 minute durations in a sealed atmospheric chamber (Figure 1d).

Figure 4 – The effect of oil concentration on the average droplet diameter of emulsions stabilized by 5.3 wt% Tween 80 and 4.4 wt% Span 80. 15mL samples were sonicated for 10 minute durations in a sealed atmospheric chamber (Figure 1d).

Figure 5 – Emulsion size (Z-average diameter) as a function of polyethylene glycol (~6000 Da) content for 15 vol% triglyceride oil emulsions stabilized by 5.6 wt% of sodium docecyl sulfate. Emulsions were prepared using a Microfluidizer, 5 passes at 1000 ± 50 Bar.

Figure 6 – Emulsion size (Z-average diameter) for a mixture of 5.6 wt% sodium dodecyl sulfate and 13.6 wt% polyethylene glycol in a 15 wt% sunflower oil/water emulsion. Emulsions were created in a range of equipment configurations.

Figure 7 – Particle size distributions (intensity weighted) for a mixture of 5.6 wt% sodium dodecyl sulfate and 13.6 wt% polyethylene glycol in an emulsion of 15 wt% sunflower oil with the balance water. Emulsions were created in the glass batch cell.

Figure 8 – The effect of increasing overpressure in the continuous flow through cell (Figure 1e) on emulsion particle size. 20mL samples of SDS-PEG emulsions (5.6 wt%

SDS and 13.6 wt% PEG in an emulsion of 15 wt% sunflower oil) were sonicated for 1 minute under varying overpressure. The general trend shows decreasing particle size as overpressure is increased. Note that no emulsification was achieved past 450kPa pressure.

Figure 9 – The relationship between the specific energy input and droplet size for a mixture of 5.6 wt% sodium dodecyl sulfate and 13.6 wt% polyethylene glycol in a 15 wt% sunflower oil/water emulsion. Emulsions were created in a range of equipment configurations and at a range of system pressures.

Figure 1

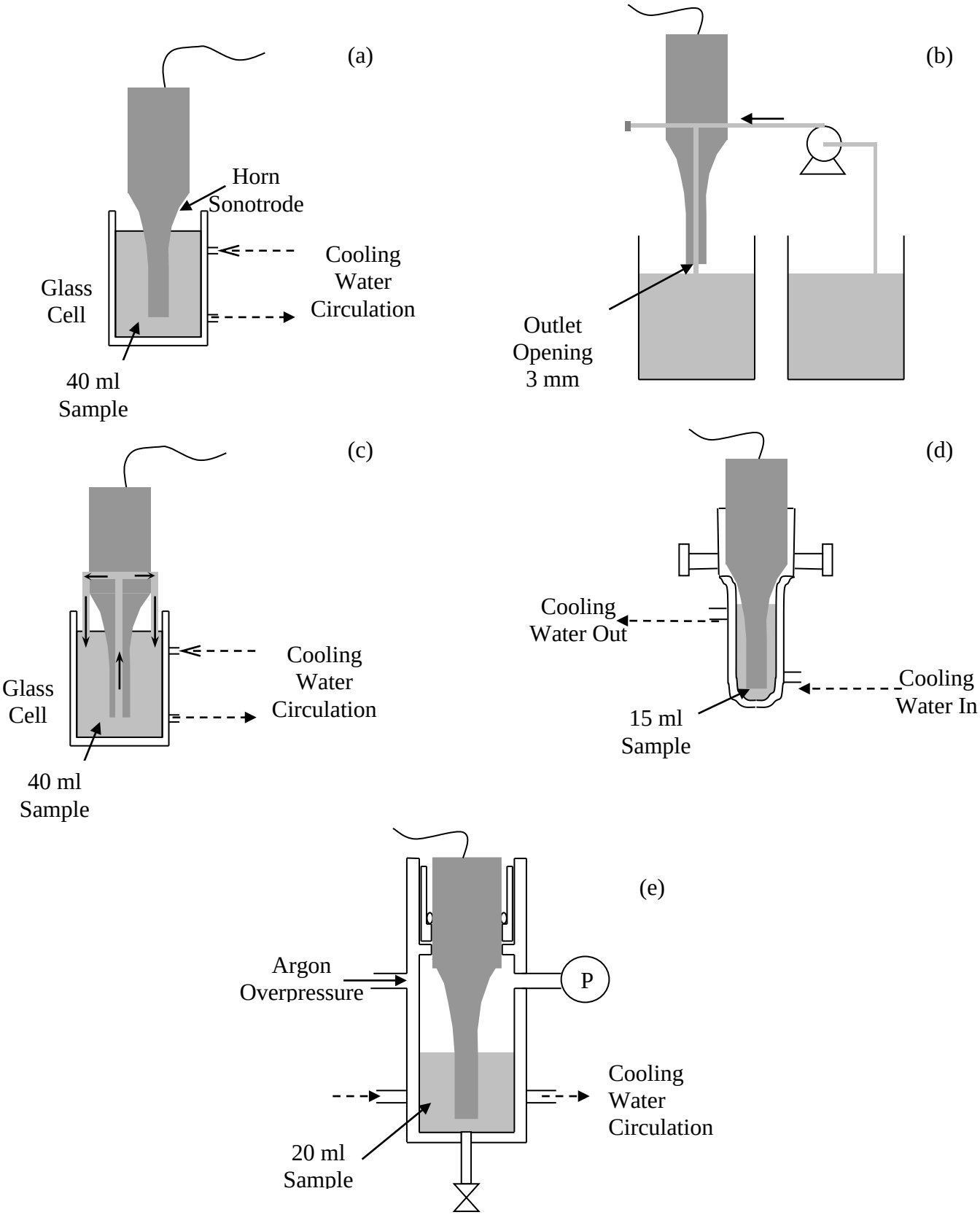
(a)
Horn
Sonotrode
Glass
Cell
Cooling
Water
Circulation
40 ml
Sample
(b)
Outlet
Opening
3 mm
(c)
Glass
Cell
Cooling
Water
Circulation
40 ml
Sample
(d)
Cooling
Water Out
Cooling
Water In
15 ml
Sample
(e)
Argon
Overpressure
P
Cooling
Water
Circulation
20 ml
Sample

Figure 2

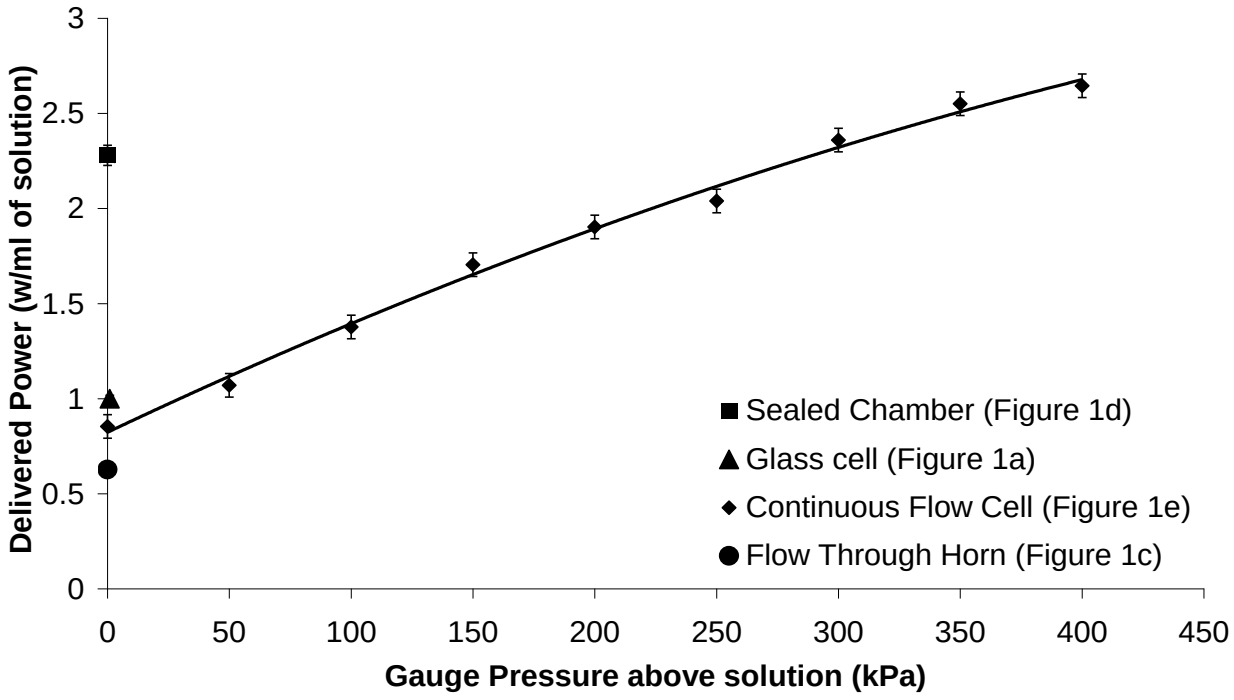
Delivered Power (w/ml of solution)
3
2.5
2
1.5
1
0.5
0
0
50
100
150
200
250
300
350
400
450
Gauge Pressure above solution (kPa)
Sealed Chamber (Figure 1d)
Glass cell (Figure 1a)
Continuous Flow Cell (Figure 1e)
Flow Through Horn (Figure 1c)

Figure 3

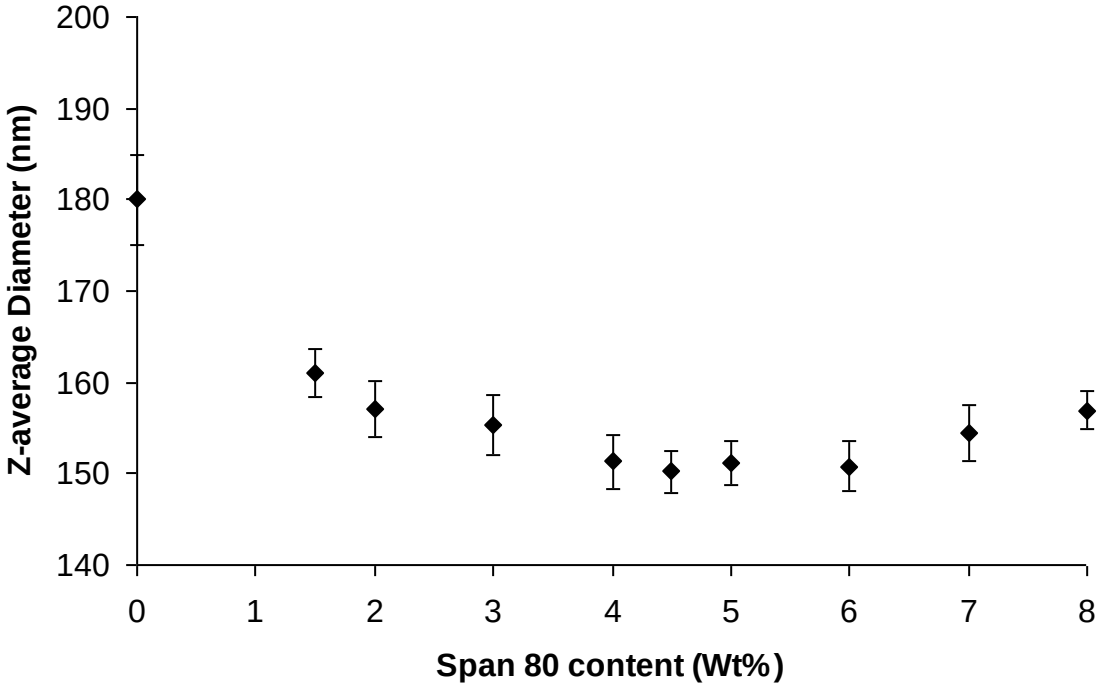
200
190
180
170
160
150
140
Z-average Diameter (nm)
0
1
2
3
4
5
6
7
8
Span 80 content (Wt%)

Figure 4

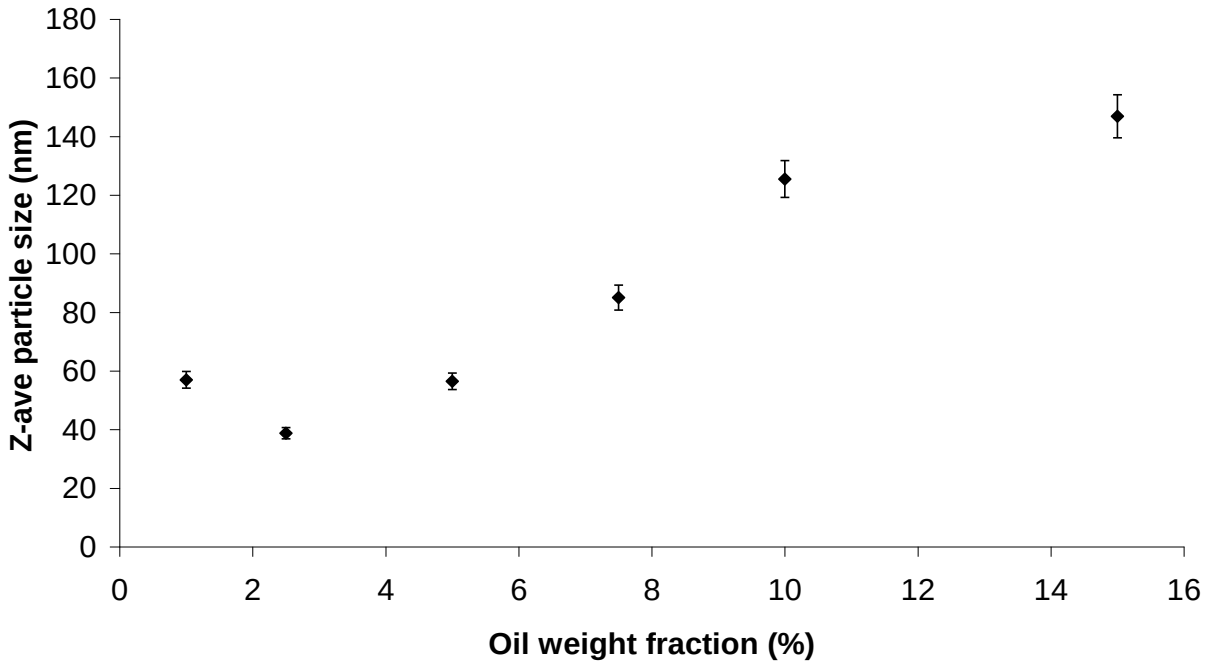
Z-ave particle size (nm)
180
160
140
120
100
80
60
40
20
0
0
2
4
6
8
10
12
14
16
Oil weight fraction (%)

Figure 5

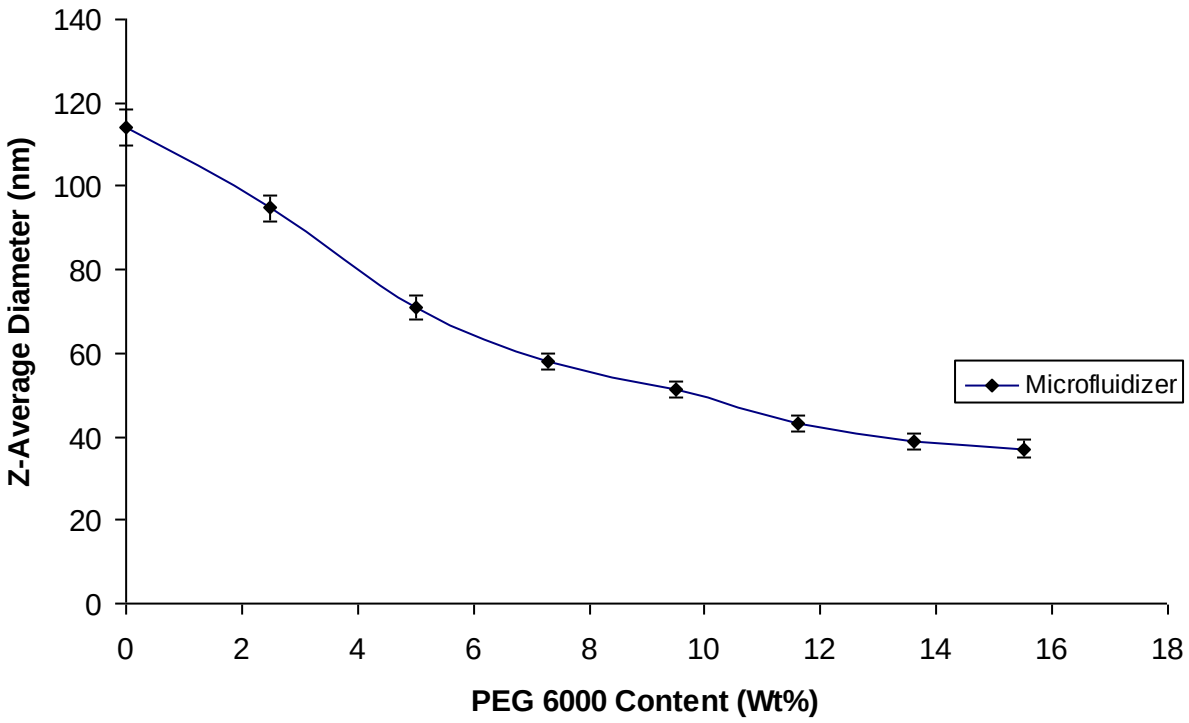
140
120
100
80
60
40
20
0
Z-Average Diameter (nm)
0
2
4
6
8
10
12
14
16
18
PEG 6000 Content (Wt%)
Microfluidizer

Figure 6

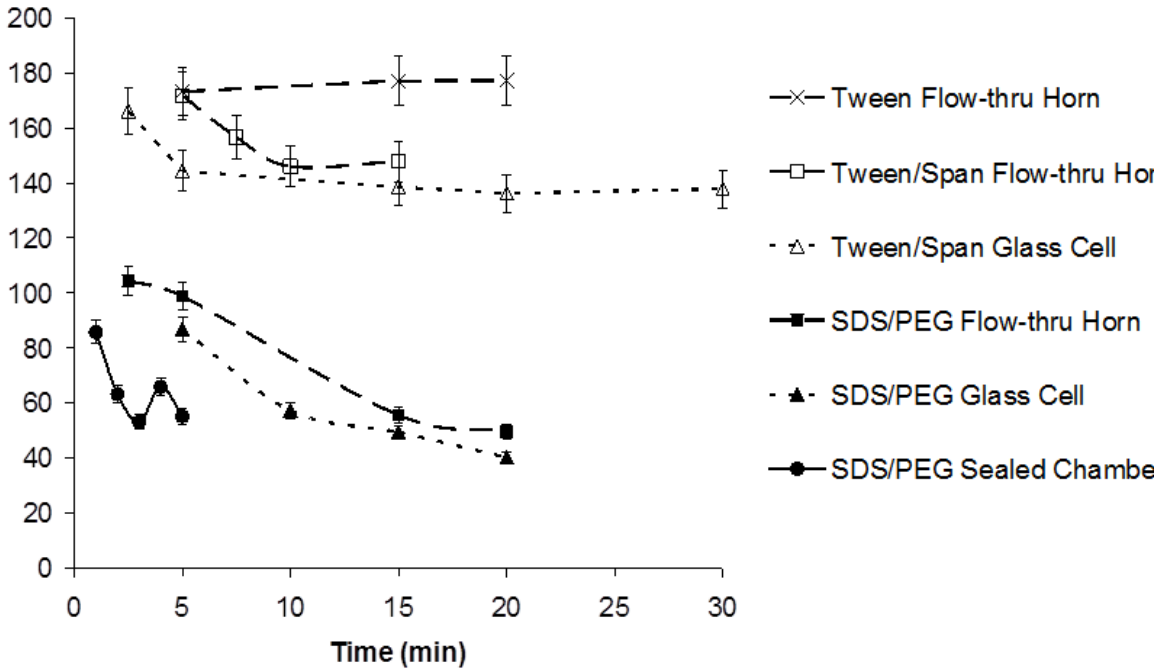
200
180
160
140
120
100
80
60
40
20
0
0
5
10
15
20
25
30
Time (min)
Tween Flow-thru Horn
Tween/Span Flow-thru Hor
Tween/Span Glass Cell
SDS/PEG Flow-thru Horn
SDS/PEG Glass Cell
SDS/PEG Sealed Chambe

Figure 7

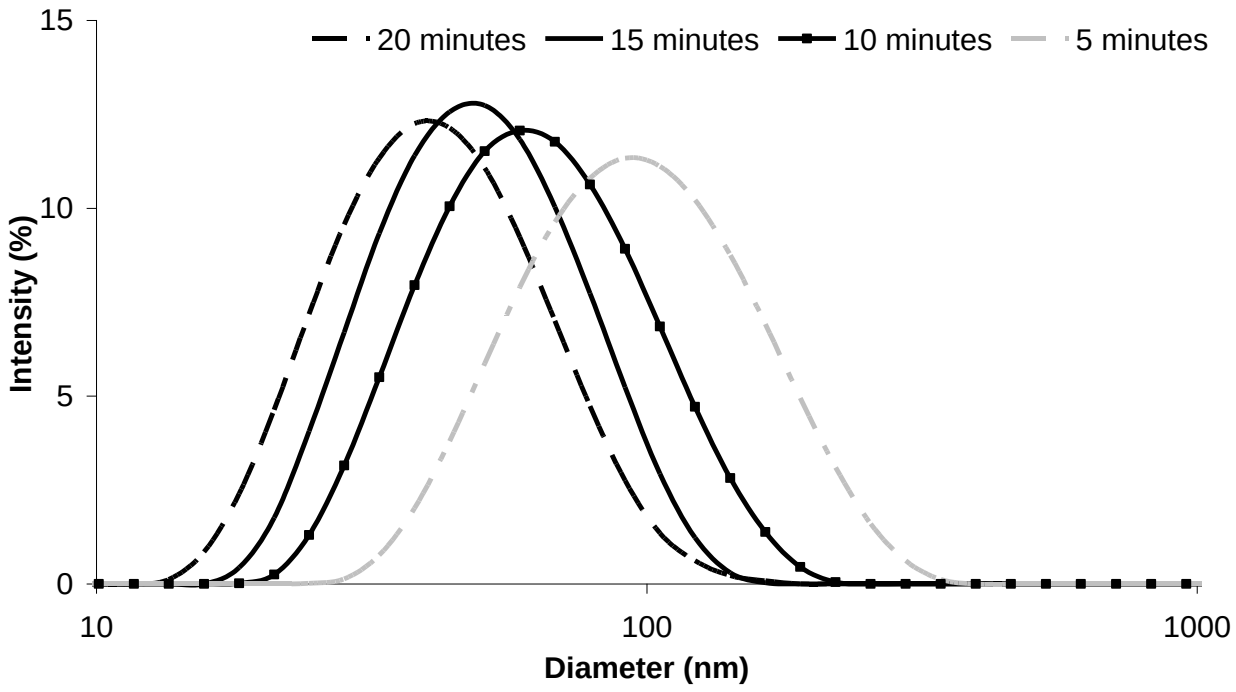
15
10
5
0
Intensity (%)
20 minutes
15 minutes
10 minutes
5 minutes
10
100
1000
Diameter (nm)

Figure 8

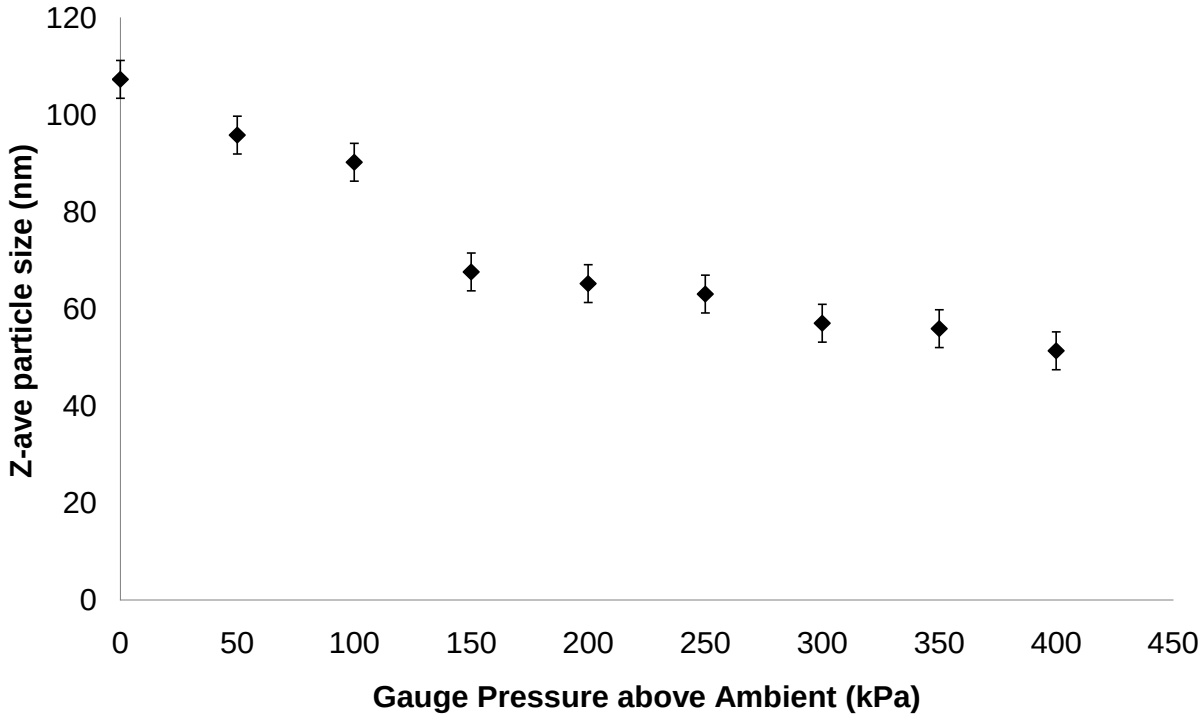
120
100
80
60
40
20
0
Z-ave particle size (nm)
0
50
100
150
200
250
300
350
400
450
Gauge Pressure above Ambient (kPa)

Figure 9

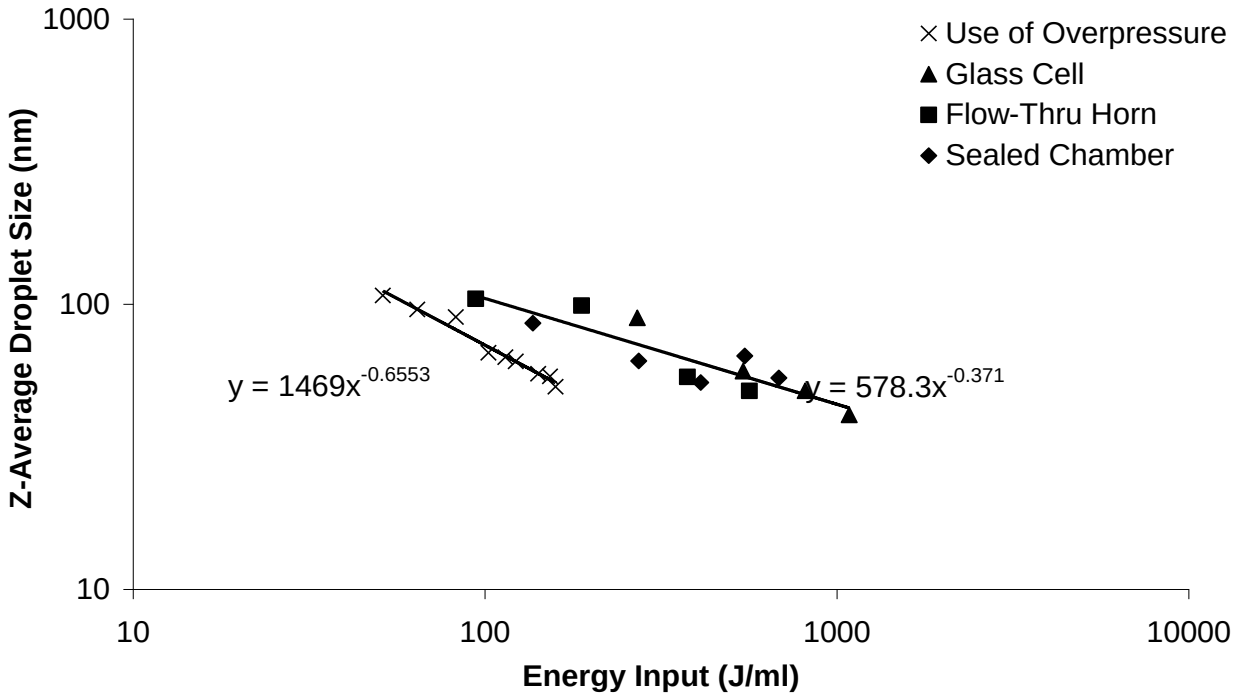
1000
100
10
Z-Average Droplet Size (nm)
10
100
1000
10000
Energy Input (J/ml)
Use of Overpressure
Glass Cell
Flow-Thru Horn
Sealed Chamber
y = 1469x-0.6553
y = 578.3x-0.371